J Kotomins et al.

Kinetics of electrons centers annealing in Al2O3 crystals

Kinetics of dimer F_2 type center annealing in Al_2O_3 crystals

V. N. Kuzovkov[1], E. A. Kotomin[1,2], A.I. Popov[1]

[1]*Institute of Solid State Physics, Kengaraga 8, Riga LV 1063, Latvia*

[2]*Max Planck Institute for Solid State Research, Heisenbergstr. 1, Stuttgart 70569, Germany*

Abstract

The experimental annealing kinetics of the primary electronic F , F^+ centers and dimer F_2 centers observed in Al_2O_3 produced under neutron irradiation were carefully analyzed. The developed theory takes into account the interstitial ion diffusion and recombination with immobile F^+ and F_2-centers, as well as mutual sequential transformation with temperature of three types of experimentally observed dimer centers which differ by net charges (0. +1, +2) with respect to the host crystalline sites. The relative initial concentrations of three types of F_2 electronic defects before annealing are obtained, along with energy barriers between their ground states as well as the relaxation energies.

*Corresponding author. Tel: +371 67187480. E-mail address: kotomin@latnet.lv (E.A. Kotomin)

1. Introduction

α-Al_2O_3 (corundum, sapphire) is important radiation-resistant material with potential applications for components of diagnostic windows and breeder blankets [1–4]. The radiation-induced vacancies in oxygen sublattice produce electronic defects (color centers) with trapped one or two electrons (the F^+ and F centers, respectively) [5,6]. The F type centers in Al_2O_3 show a distinctive optical absorption: at 203 nm (6.1 eV) (F centers) and 256 nm (4.8 eV) (F^+ centers). Properties of complementary interstitial impurity atoms O_i are much less known due to absence of magnetic moment and optical absorption in a suitable energy range. It is known, however, that in most binary oxides (as well as in alkali halides) [7] the anion interstitials are considerably more mobile than complementary vacancies and thus the F-type center annealing at intermediate temperatures (in MgO and Al_2O_3 around 400-500 K) arises due to the recombination of *immobile* electron centers with mobile interstitials. This is supported by the fact that F center aggregation in thermochemically reduced MgO [8-10] and Al_2O_3 [11] (when only F centers exist) occurs at very high temperatures, typically above 1500 K.

Under intensive neutron irradiation, along with single defects, dimer F_2 electron centers are also observed [12, 13]. These defects consist of two nearest oxygen vacancies trapped different number of electrons [5,6] which is confirmed by theoretical calculations [14]. Three types of F_2 centers reveal optical absorption at 302 nm (4.1 eV), 356 nm (3.5 eV) and 450 nm (2.7 eV) [11-13]. Study of the F- and F_2-center annealing is important for prediction and control of radiation stability of oxide materials. Recently, we developed phenomenological theory describing the diffusion-controlled kinetics of radiation defect annealing in ionic solids [15,16] and demonstrated how analysis of the experimental data allows us to extract two control parameters: the migration energy of the interstitial ions E_a and pre-factor $X = N_0RD_0/\beta$, where N_0 is initial defect concentration,   R recombination radius, D_0 diffusion pre-exponent, and β heating rate.

In this paper, we analyzed available experimental kinetics of the single F- and dimer F_2 type center annealing in Al_2O_3 in a wide temperature range (300-1200 K).

2. Results

2.1. The *F* centers

The results of theoretical analysis [15,16] of the *F*-type center annealing in Al_2O_3 irradiated by neutrons under very different conditions are summarised in Table 1, whereas Fig.1 shows theoretical fitting for cases 1 to 6. As follows from a legend in Table 1, experimental conditions were quite different (both neuton energies and fluxes).

Table 1. The explanation of curves 1-6 in Fig.1 and the obtained migration energy of interstitial oxygen ions E_a and pre-exponential factor X under different radiation conditions (Nr.1-10).

Nr.	Type	E_a (eV)	X (K^{-1})	Legend	Reference
1	F	0.79	$2.1x10^1$	Undoped crystals were irradiated up to a dose of $2.16x10^{17}n/cm^2$ and containing comparable amounts of F and F^+ centers ($3.6x10^{17}$ and $2.5x10^{16}cm^{-3}$	[17]
2	F^+	0.89	$7.0x10^1$	same as 1	[17]
3	F^+	0.40	$2.3x10^{-1}$	Samples were irradiated at 400 K up to 5x1018, 1019, 2x1021 and I022n m^{-2}, in the spallation neutron source	[2]
4	F^+	0.47	$1.2x10^0$	The fluence of fast neutron (En > 1.2 MeV) was in the range of $4.4x10^{16}$– $1.4x10^{18}$ n /cm^2. After irradiation, thermal annealing was performed for 15 min at increasing temperatures in air. The heat treatment is performed on sample irradiated at $9.1x10^{17}$ n /cm^2 from room temperature to 900 C. After irradiation at $4.4x10^{16}$ n/cm^2, only 203 and 255 nm absorption bands are clearly observed. With increasing fluence, 203 nm absorption band saturate at $1.3x10^{17}$ n/cm^2 and others absorption bands appear at 300, 357 and 450 nm.	[13], Fig.5
5	F^+	0.39	$5.3x10^{-1}$	Several bands (302, 356, 384, 450, and 570nm bands) are observed irradiation to a dose of above 10^{17} fast neutron/cm^2.	[12], Fig.3
6	F^+ 4.85eV= 256nm	0.27	$4.0x10^{-1}$	Single-crystal Al2O3 were irradiated at room temperature at a flux of 10^{12} n/cm^2 s to a fluence of 10^{17} n/cm^2. 14-MeV and fission-neutron damage are qualitatively similar, although the 14-MeV neutrons are 4 times as effective in causing damage.	[18], Fig.2c
7	F 6.02eV =206nm	0.22	$3.3x10^{-2}$	Same as 6	[18], Fig.2a
8	F	0.17	$1.3x10^{-2}$	Isochronal decay of the **F** centers. The samples were irradiated to a dose of $4x10^{16}$ fast neutrons/cm^2 at -250 C and annealed for 5 min. In this case, only the F and F+ bands were	[12], Fig.2

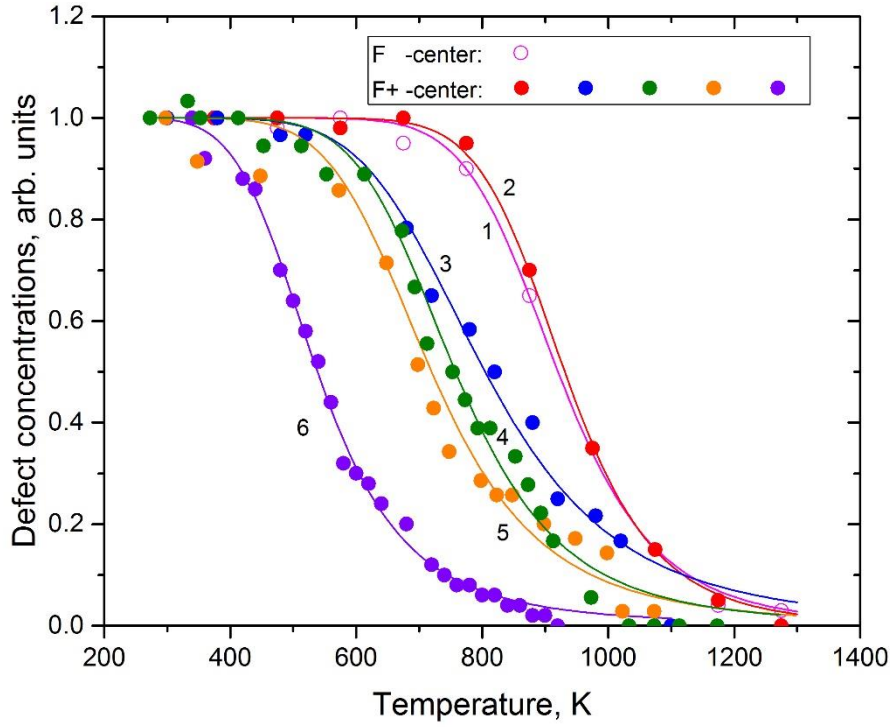|				detected.	
9	F	0.14	1.9×10^{-3}	Isochronal annealing behavior of F-centers. Pure Al2O3 single crystal has been irradiated with fast neutron (En > 1.2 MeV) fluence of about 4×10^{16} n/cm^2 . After irradiation, thermal annealing was performed for 15 min at increasing temperatures in air up to 1173 K.	[19], Fig.3
10	F^+	0.35	1.4×10^{0}	Isochronal thermal anneal of the 4.8 eV F band in Al_2O_3: fission-spectrum neutrons.	[11], Fig.12b

Fig.1. The kinetics of the *F* or *F*$^+$ center annealing for different neutron fluxes (see Table 1 for details).

The first conclusion confirms our preliminary results [15] on a strong dependence of the E_a, X parameters on the irradiation flux: Decrease of the diffusion energies is accompanied by decrease, by orders of magnitude, of the pre-exponential factors. Moreover, pre-exponential factors X are typically much smaller than its simple estimate for normal diffusion in crystals (assuming $N_0 = 10^{17}$ cm^{-3}, R= 10 Å, $D_0 = 10^{-3}$ cm^2 s^{-1}, $\beta = 10$ K/min, one expects the X= 10^8 K^{-1}). We believe that this is result of increasing material disordering with larger and larger fluences which is supported by recent experimental studies [20] and discussed in detail in oncoming paper [21]. The smallest fluxes correspond to curves 1 and 2 (the *F* and *F*$^+$ centers), which show the largest O_i migration energies (0.8-0.9 eV) and largest pre-factors X=20-70 K^{-1}. This migration energy is indeed close to theoretically calculated value for the *charged*

interstitial ions [22], and considerably smaller than the estimate for the neutral interstitial [23]. Note that the calculated migration energy of the electronic F centers is much larger, 4.5 eV [15], therefore, these defects are immobile at the temperature range shown in Fig.1.

Second, the annealing curves for the F and F^+ centers (curves 1 and 2 in Fig.1) decay sinchronously which means that no transformation $F \rightarrow F^+$ occurs; both defects recombine independently with mobile interstitials. The difference of 0.1 eV in the obtained migration energies could serve as estimate of our theory accuracy.

 2.2. Dimer centers

In this Section, we discuss the annealing of the dimer F_2 center kinetics observed in two experimental studies [12,13]. As is seen in Fig.1, curves 4 and 5 for the F^+ centers in these experiments decay smoothly and show no peculiarities due to presence of dimer defects, due to dimer relatively small concentrations. Following original papers, Fig.2 shows the normalized annealing kinetics of the three F_2- centers from ref. [12] whereas these kinetics were not normalized in ref. [13]. (In our analysis we normalized data [13] for analysis and returned them back to original form in Fig.3). Note that this is generally believed (e.g. [12,13]) that three types of the dimer centers are created as the result of bimolecular reactions between single mobile vacancies, e.g. $F + F \rightarrow F_2$, $F + F^+ \rightarrow F_2^+$ and $F^+ + F^+ \rightarrow F_2^{2+}$. However, we understand now that the F-centers are immobile at the relevant temperatures and thus mutual transformation of the dimer centers is electronic process controlled by electrons thermal ionization from vacancies and re-trapping by other vacancies. Essentially, the F_2 type centers observed [12,13] were created during the irradiation (e.g. as a result of overlap of tracks produced by neutrons) but not sample annealing. In parallel, the total F_2 concentration decreases, as well as that for the single defects, due to recombination with the mobile interstitials.

Let us analyze now data in Fig.2, and denote F_2 centers in the sequence of their appearance: F_2 (1) corresponds to the peak at 302 nm, $F_2(2)$ 450 nm, $F_2(3)$ 356 nm. As one can see, concentration of the single F centers monotonous decreases (see Fig. 1, curve (5)) whereas three dimer centers show very different behavior: similar but faster monotonous decay of $F_2(1)$, a sharp $F_2(2)$ peak in the temperature range of the $F_2(1)$ decay, and $F_2(3)$ peak at higher temperatures where $F_2(2)$ centers decay.
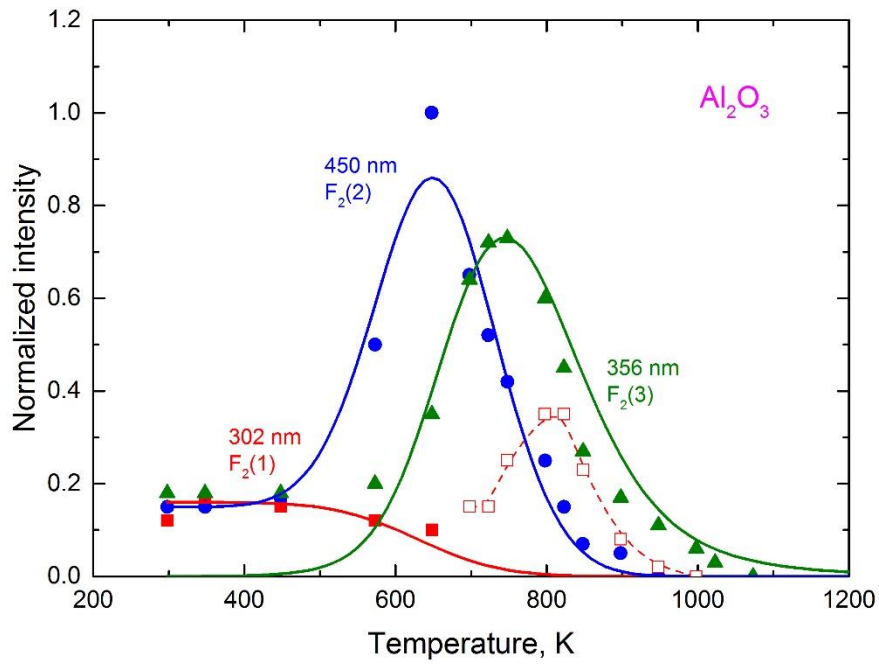
Fig.2. Experimental points from ref. [12] and their theoretical analysis (full lines). Maximum of the 450 nm band intensity was normalized to unity. Background was substracted and peaks normalized. Empty red squares very likely do not related to the F2(1) band (e.g. see discussion in Ref. [13], p.2990, for more details) and were neglected in our analysis.
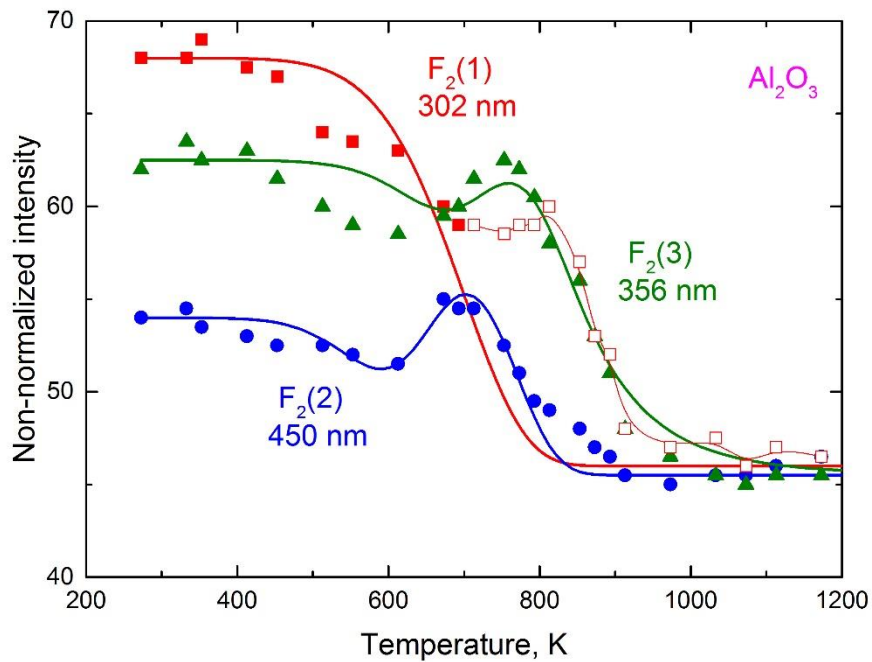
Fig.3. Non-normalized experimental points from ref.[13] and their theoretical analysis (full lines).

This supports idea of mutual transformation of three types of dimer centers. The fact that the F center decay is not affected by the mentioned peculiarities in the F_2 kinetics indicates at negligible concentration of dimer centers compared to that of the F centers. This allows us to treat kinetics of the F and F_2 centers independently which greatly simplifies the problem. In particular, while considering the kinetics of dimer centers, the concentration of hole centers could be taken from solution for the kinetics for single centers.

As mentioned above, the annealing kinetics of dimer centers is a combination of the two independent processes: recombination of immobile electron centers with mobile interstitials (hole centers) and mutual transformation of three types of F_2-type centers: $F_2(1) \rightarrow F_2(2)$, and $F_2(2) \rightarrow F_2(3)$. Let us introduce the dimensionless defect concentrations: $C_F(t) = n(t)/n(0)$. It could be shown that total concentration of dimer centers is defined by the singe center decay kinetics as $C_F(t)^\kappa$, где $\kappa = R_2/R$, R and R_2 are recombination radii for interstitials with single and dimer centers. Three dimers could be characterized by relative concentrations (probabilities) $W_i(t)$, i=1,2,3, with the normalization $W_1(t) + W_2(t) + W_3(t) = 1$ and initial condition $W_i(0) = w_i$. The dimer concentrations are defined as products $W_i(t)C(t)^\kappa$. These concentrations were rescaled in Fig.2, following data presentation in ref.[13].

The probabilities to find three types of centers are defined by the following set of kinetic equations:

$$\frac{d W_1(t)}{dt} = -p_1 W_1(t) , \tag{1}$$

$$\frac{d W_2(t)}{dt} = p_1 W_1(t) - p_2 W_2(t), \tag{2}$$

$$\frac{d W_3(t)}{dt} = p_2 W_2(t). \tag{3}$$

These equations describe dimer center mutual transformations, $F_2(1) \rightarrow F_2(2)$ with the rate $p_1 = p_1^0 \exp(-E_b/k_B T)$, and then $F_2(2) \rightarrow F_2(3)$ (with the rate $p_2 = p_2^0 \exp(-E_c/k_B T)$). The equation was numerically solved, provided the constant heating rate $\beta(t) = \beta = $ const. Using the least square method, we obtained the main kinetic parameters –

activation energies E_b and E_c, two pre-exponents $P_1=p_1^0/\beta$ and $P_2=p_2^0/\beta$, recombination parameter κ and initial defect populations w_i.

The results are shown in Fig.2 and Fig.3 in full curves and summarized in Table 2. As one can see, a simple model describes very well a whole set of experimental data.

Table 2. The obtained parameters of mutual dimer center transformations.

| Ref. | F centers diffusion | | F_2 center mutual transformation | | | | | | |
| | Activation energy | Pre-exponent | Activation enegies | | Pre-exponents | | Populations | | |
	E_a , eV	X , K^{-1}	E_b ,eV	E_c ,eV	P_1 , K^{-1}	P_2 , K^{-1}	W_1	W_2	W_3
[12]	0.39	$5.3 \cdot 10^{-1}$	0.46	0.32	$9.7 \cdot 10^0$	$4.3 \cdot 10^0$	0.99	0.01	0.00
[13]	0.47	$1.2 \cdot 10^0$	0.87	0.47	$9.5 \cdot 10^3$	$1.6 \cdot 10^2$	0.78	0.02	0.20

The parameter $\kappa=2.06$ [12] and 1.66 [13]

The calculated activation energies for mutual center transformations based on data [12] are similar, $E_b=0.46$ eV and $E_c=0.32$ eV and close to the Oi migration energy $E_a=0.39$ eV, three related pre-exponents are also close: $X=5.3 \cdot 10^{-1}$ K^{-1}, $P_1=9.7 \cdot 10^0$ K^{-1} and $P_2=4.3 \cdot 10^0$ K^{-1}. The parameter $\kappa=2.06$ is close to the ratio of geometric cross sections of a single and di-vacancy. Lastly, the initial $F_2(1)$ dimer population is predominant, $w_1=0.992$, whereas that for $F_2(2)$ is very small, and negligible for $F_2(3)$.

The analysis of data [13] demonstrates that transformation energies are slightly larger than in ref.[12]: $E_b=0.87$ eV and $E_c=0.47$ eV, as well as O_i migration energy $E_a=0.47$ eV. Three related pre-exponents are also close: $X=1.2 \cdot 10^0$ K^{-1}, $P_1=9.5 \cdot 10^3$ K^{-1} and $P_2=1.6 \cdot 10^2$ K^{-1}. The parameter $\kappa=1.66$ is again close to the ratio of geometric cross sections of a single and di-vacancy. Lastly, the initial $F_2(1)$ dimer populations is large, $w_1=0.78$, $F_2(2)$ dimer populations is very small, $w_2=0.02$, whereas population of the third dimer is intermediate, $w_3=0.20$. At any rate, $F_2(1)$ dimers again are predominant defects after irradiation and before annealing.

Temperature evolution of three types of dimer concentrations in both experiments [12,13] is shown in Figs. 4 and 5. It is well seen here that the main difference lies in the larger initial concentration of $F_2(3)$ dimers under experimental conditions of ref. [13] but qualitatively results are very similar.

It could be assumed that mutual transformation of three F_2-type centers correspond to three possible dimer charges: F_2, F_2^+ and F_2^{2+} (four, three and two trapped electrons

in the di-vacancy (see Fig. 3 [24], Fig. 3 [14]) which occurs via *electronic* process -- dimers successive thermal ionization with release each time one electron, $F_2 \rightarrow F_2^+ + e$ and $F_2^+ \rightarrow F_2^{2+} + e$, respectively. This hypothesis needs further careful analysis.
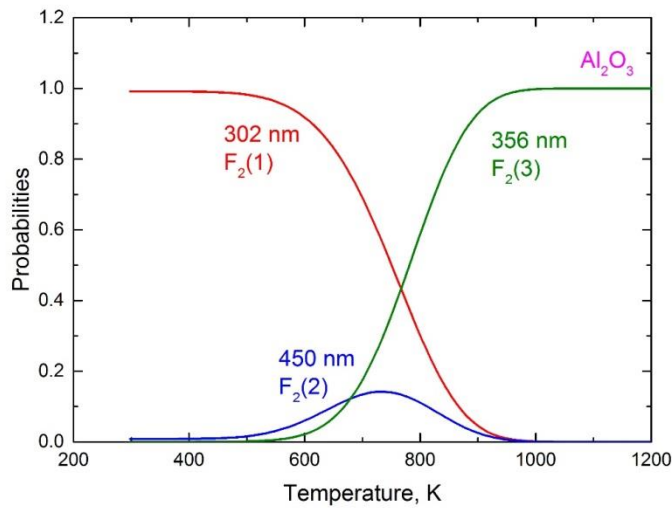

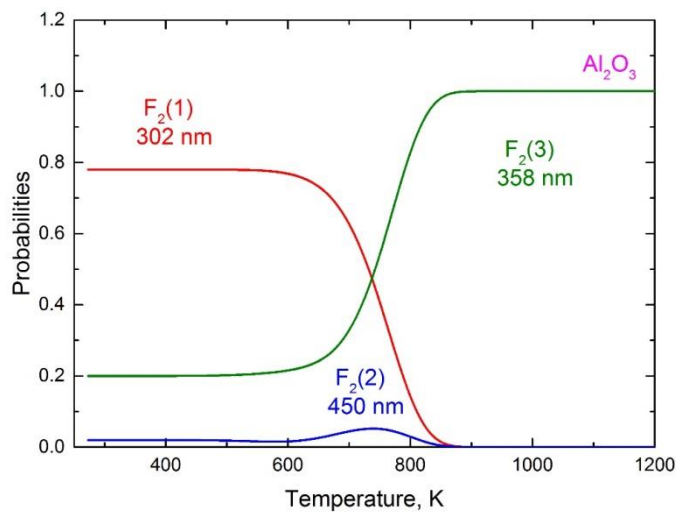Fig.4. The calculated temperature dependence of dimer center populations [12].

Fig.5. same as Fig.4 for data in ref.[13].

3. Conclusions

Phenomenological theory of the diffusion-controlled annealing kinetics of single and dimer electron centers in irradiated oxides was developed and applied to Al_2O_3 crystals. Theoretical analysis of the available experimental kinetics for the *F* type

centers produced under neutron irradiation shows strong dependence of the migration energy and pre-exponent for oxygen interstitial ions on the radiation fluence which is ascribed to increasing material disordering and will be discussed in oncoming paper [21]. The migration energy of 0.8 eV for lowest fluence (almost perfect crystal) is in a good agreement with theoretical prediction for *charged* oxygen interstitials in crystalline matrix [19].

Analysis of the kinetics of the mutual transformation of three types of dimer F_2-type centers observed under intensive neutron irradiation [12,13] allows us to extract all kinetic parameters and supports the idea that these three centers differ by the charge states (neutral, single- and double-charged defects with respect to the perfect crystal). We suggest the following center interpretation: 302 nm - F_2, 450 nm - F_2^+ , and 356 nm F_2^{2+}. Note, that determination of the defect charge states is very non-trivial problem; there is also no unique opinion in the literature also for F_2-type dimer centers, which needs further analysis. The general hypothesis of different charge states and electronic processes behind their mutual transformations is supported by our similar results for three types of dimer centers in MgF_2 [25] to be discussed elsewhere [26]. It is also clearly shown here that this transformation does not involve migration of single F-type centers but likely electron thermal ionization and delocalization between dimer centers.

Acknowledgments

References

1. J. Valbis, N. Itoh, Electronic excitations, luminescence and lattice defect formation in α-Al_2O_3 crystals. Radiat. Eff. Defects Solids 116 (1991) 171–189.
2. R. Vila, A. Ibarra, M. de Castro, F.W. Clinard, Thermally stimulated

depolarization currents in neutron-irradiated Al_2O_3. Solid St. Comm. **79** (1991) 295-297.

3. F. Mota, C.J. Ortiz, R. Vila, N. Casal, A. Garcia, A. Ibarra, Calculation of damage function of Al_2O_3 in irradiation facilities for fusion reactor applications. J. Nucl. Mater. **442** (Suppl. 1) (2013) 5699-5704.

4. A. Serikov, L. Bertalot, M. Clough, U. Fischer, A. Suarez, Neutronics analysis for ITER cable looms. Fusion Eng. Des. **96–97** (2015) 943–947.

5. E.A. Kotomin, A.I. Popov, Radiation-induced point defects in simple oxides. Nucl. Instrum. Meth. Phys. Res. B **141** (1998) 1-15 (a review article)

6. A.M. Stoneham, *Theory of Defects in Solids*, Oxford, 1975; N. Itoh and A.M. Stoneham, *Material Modification by Electronic Excitations*, 2001.

7. A. Lushchik, Ch. Lushchik, K. Schwartz, E. Vasil'chenko, T. Kärner, I. Kudryavtseva, V. Issakhanyan, A. Shugai, Stabilization and annealing of interstitials formed by radiation in binary metal oxides and fluorides. Nucl. Instrum. Meth. Phys. Res. B **266** (2008) 2868–2871.

8. M.A. Monge, A.I. Popov, C. Ballesteros, R. González, Y. Chen, E.A. Kotomin, Formation of anion vacancy cluster and nano cavities in thermochemically reduced MgO single crystals. Phys. Rev. B **62** (2000) 9299-9304.

9. A.I. Popov, M.A. Monge, R. González, Y. Chen, E.A. Kotomin, Dynamics of *F*-center annihilation in thermochemically reduced MgO single crystals. Solid State Commun. **118** (2001) 163-167.

10. E.A. Kotomin, A.I. Popov, In: *Radiation Effects in Solids*, NATO Science Series II-Mathematics Physics and Chemistry (E. Kotomin, K.Sikafus eds.), **235** (2007) 153–192

11. B.D. Evans, A review of the optical properties of anion lattice vacancies, and electrical conduction in α-Al_2O_3: their relation to radiation-induced electrical degradation. J. Nucl. Mater. **219** (1995) 202-223 (review article)

12. K. Atobe, N. Ishimoto, and M. Nakagawa, Irradiation-Induced Aggregate Centers in Single Crystal Al_2O_3. Phys. Stat. Sol. (a), **89** (1985) 155.

13. M. Izerrouken and T. Benyahia, Absorption and photoluminescence study of Al_2O_3 single crystal irradiated with fast neutrons, Nucl. Instrum. Meth. Phys. Res. B **268** (2010) 2987–2990.

14. E.A. Kotomin, A. Stashans, L.N. Kantorovich, A.I. Lifshitz, A.I. Popov, I.A. Tale, J.-L. Calais, Calculations of the geometry and optical properties of F_{Mg} and dimer (F_2 type) centers in corundum crystals. Phys. Rev. B **51** (1995) 8770-8779.

15. E.A. Kotomin, V.N. Kuzovkov, A.I. Popov, and R. Vila, Kinetics of *F* center annealing and colloid formation in Al_2O_3. - Nucl. Instr. Meth. Phys. Res. B, 2016, **374**, 107–110.

16. V.N. Kuzovkov, A.I. Popov, E.A. Kotomin, A.M. Moskina, E. Vasil'chenko, and A. Lushchik, Theoretical analysis of the kinetics of low-temperature defect recombination in alkali halide crystals. - Low Temp. Phys., 2016, **42**, 748-755.

17. R. Ramírez, M. Tardío, R. González, J.E. Muñoz Santiuste, M.R. Kokta. Optical properties of vacancies in thermochemically reduced Mg-doped sapphire single crystals. J. Appl. Phys. 101 (2007) 123520 (1-12).

18. J. M. Bunch, F. W. Clinard JR. Damage of Single-Crystal Al_2O_3 by 14-MeV Neutrons, Journal of The American Ceramic Society, 57 (1974) 279-280

19. M. Izerrouken, Y. Djouadi, H. Zirour. Annealing process of F- and F+-centers in Al_2O_3 single crystal induced by fast neutrons irradiation. Nucl. Instrum. Meth. Phys. Res. B **319** (2014) 29–33.

20. C.Grygiel, F. Moisy, M. Sall, H. Lebius, E. Balanzat, T. Madi, T. Been, D. Marie, I. Monnet. In situ kinetics of modifications induced by swift heavy ions in Al2O3: color center formation, structural modification and amorphization. Nucl. Instrum. Meth. Phys. Res. B (2017), in press

21. V.N. Kuzovkov, E.A. Kotomin, A.I.Popov, J. Maier. xxxx (2017), in preparation

22. A. Platonenko, D. Gryaznov, Yu.F. Zhukovskii, E.A. Kotomin, *Ab initio* simulations on charged interstitial oxygen migration in corundum. Nucl. Instrum. Meth. Phys. Res. B (2017), submitted

23. Yu.F. Zhukovskii, A. Platonenko, S. Piskunov, E.A. Kotomin, *Ab initio* simulations on migration paths of interstitial oxygen in corundum. Nucl. Instrum. Meth. Phys. Res. B **374** (2016) 29-34.

24. B.D. Evans, Optical properties of lattice defects in α-Al_2O_3. Nucl. Instr. and Meth. B **91** (1994) 258-262.

25. A.S. El-Said, R. Neumann, K. Schwartz, C. Trautmann. Swelling and creation of color centers in MgF_2 single crystals irradiated with energetic heavy ions. Nucl. Instrum. Meth. Phys. Res. B **245** (2006) 250–254.

26. V.N. Kuzovkov, E.A.Kotomin, A.I. Popov, Kinetics of dimer F_2 type center annealing in MgF_2 crystals. Nucl. Instrum. Meth. Phys. Res.. B, 2017, submitted